BABAR-CONF-09/001
SLAC-PUB-13543
February 2009

Search for Dimuon Decays of a Light Scalar in Radiative Transitions $\Upsilon(3S) \to \gamma A^0$

The *BABAR* Collaboration

February 12, 2009

Abstract

The fundamental nature of mass is one of the greatest mysteries in physics. The Higgs mechanism is a theoretically appealing way to account for the different masses of elementary particles and implies the existence of a new, yet unseen particle, the Higgs boson. We search for evidence of a light scalar (*e.g.* a Higgs boson) in the radiative decays of the narrow $\Upsilon(3S)$ resonance: $\Upsilon(3S) \to \gamma A^0$, $A^0 \to \mu^+\mu^-$. Such an object appears in extensions of the Standard Model, where a light *CP*-odd Higgs boson naturally couples strongly to b-quarks. We find no evidence for such processes in a sample of 122×10^6 $\Upsilon(3S)$ decays collected by the *BABAR* collaboration at the PEP-II B-factory, and set 90% C.L. upper limits on the branching fraction product $\mathcal{B}(\Upsilon(3S) \to \gamma A^0) \times \mathcal{B}(A^0 \to \mu^+\mu^-)$ at $(0.25 - 5.2) \times 10^{-6}$ in the mass range $0.212 \leq m_{A^0} \leq 9.3\,\mathrm{GeV}$. We also set a limit on the dimuon branching fraction of the η_b meson $\mathcal{B}(\eta_b \to \mu^+\mu^-) < 0.8\%$ at 90% C.L. The results are preliminary.

Submitted to Aspen 2009 Winter Conference, February 8—14, 2009, Aspen, CO

SLAC National Accelerator Laboratory, Stanford University, Stanford, CA 94309

Work supported in part by Department of Energy contract DE-AC02-76SF00515.

B. Aubert, Y. Karyotakis, J. P. Lees, V. Poireau, E. Prencipe, X. Prudent, and V. Tisserand
Laboratoire d'Annecy-le-Vieux de Physique des Particules (LAPP), Université de Savoie, CNRS/IN2P3, F-74941 Annecy-Le-Vieux, France

J. Garra Tico and E. Grauges
Universitat de Barcelona, Facultat de Fisica, Departament ECM, E-08028 Barcelona, Spain

M. Martinelli, A. Palano[ab], and M. Pappagallo[ab]
INFN Sezione di Bari[a]; Dipartmento di Fisica, Università di Bari[b], I-70126 Bari, Italy

G. Eigen, B. Stugu, and L. Sun
University of Bergen, Institute of Physics, N-5007 Bergen, Norway

M. Battaglia, D. N. Brown, L. T. Kerth, Yu. G. Kolomensky,
G. Lynch, I. L. Osipenkov, E. Petigura, K. Tackmann, and T. Tanabe
Lawrence Berkeley National Laboratory and University of California, Berkeley, California 94720, USA

C. M. Hawkes, N. Soni, and A. T. Watson
University of Birmingham, Birmingham, B15 2TT, United Kingdom

H. Koch and T. Schroeder
Ruhr Universität Bochum, Institut für Experimentalphysik 1, D-44780 Bochum, Germany

D. J. Asgeirsson, B. G. Fulsom, C. Hearty, T. S. Mattison, and J. A. McKenna
University of British Columbia, Vancouver, British Columbia, Canada V6T 1Z1

M. Barrett, A. Khan, and A. Randle-Conde
Brunel University, Uxbridge, Middlesex UB8 3PH, United Kingdom

V. E. Blinov, A. D. Bukin,* A. R. Buzykaev, V. P. Druzhinin, V. B. Golubev,
A. P. Onuchin, S. I. Serednyakov, Yu. I. Skovpen, E. P. Solodov, and K. Yu. Todyshev
Budker Institute of Nuclear Physics, Novosibirsk 630090, Russia

M. Bondioli, S. Curry, I. Eschrich, D. Kirkby, A. J. Lankford, P. Lund, M. Mandelkern, E. C. Martin, and D. P. Stoker
University of California at Irvine, Irvine, California 92697, USA

S. Abachi and C. Buchanan
University of California at Los Angeles, Los Angeles, California 90024, USA

H. Atmacan, J. W. Gary, F. Liu, O. Long, G. M. Vitug, Z. Yasin, and L. Zhang
University of California at Riverside, Riverside, California 92521, USA

V. Sharma
University of California at San Diego, La Jolla, California 92093, USA

C. Campagnari, T. M. Hong, D. Kovalskyi, M. A. Mazur, and J. D. Richman
University of California at Santa Barbara, Santa Barbara, California 93106, USA

T. W. Beck, A. M. Eisner, C. A. Heusch, J. Kroseberg, W. S. Lockman,
A. J. Martinez, T. Schalk, B. A. Schumm, A. Seiden, and L. O. Winstrom
University of California at Santa Cruz, Institute for Particle Physics, Santa Cruz, California 95064, USA

C. H. Cheng, D. A. Doll, B. Echenard, F. Fang, D. G. Hitlin, I. Narsky, T. Piatenko, and F. C. Porter
California Institute of Technology, Pasadena, California 91125, USA

R. Andreassen, G. Mancinelli, B. T. Meadows, K. Mishra, and M. D. Sokoloff
University of Cincinnati, Cincinnati, Ohio 45221, USA

P. C. Bloom, W. T. Ford, A. Gaz, J. F. Hirschauer, M. Nagel, U. Nauenberg, J. G. Smith, and S. R. Wagner
University of Colorado, Boulder, Colorado 80309, USA

R. Ayad,[†] A. Soffer,[‡] W. H. Toki, and R. J. Wilson
Colorado State University, Fort Collins, Colorado 80523, USA

E. Feltresi, A. Hauke, H. Jasper, T. M. Karbach, J. Merkel, A. Petzold, B. Spaan, and K. Wacker
Technische Universität Dortmund, Fakultät Physik, D-44221 Dortmund, Germany

M. J. Kobel, R. Nogowski, K. R. Schubert, R. Schwierz, and A. Volk
Technische Universität Dresden, Institut für Kern- und Teilchenphysik, D-01062 Dresden, Germany

D. Bernard, G. R. Bonneaud, E. Latour, and M. Verderi
Laboratoire Leprince-Ringuet, CNRS/IN2P3, Ecole Polytechnique, F-91128 Palaiseau, France

P. J. Clark, S. Playfer, and J. E. Watson
University of Edinburgh, Edinburgh EH9 3JZ, United Kingdom

M. Andreotti[ab], D. Bettoni[a], C. Bozzi[a], R. Calabrese[ab], A. Cecchi[ab], G. Cibinetto[ab], E. Fioravanti, P. Franchini[ab], E. Luppi[ab], M. Munerato, M. Negrini[ab], A. Petrella[ab], L. Piemontese[a], and V. Santoro[ab]
INFN Sezione di Ferrara[a]; Dipartimento di Fisica, Università di Ferrara[b], I-44100 Ferrara, Italy

R. Baldini-Ferroli, A. Calcaterra, R. de Sangro, G. Finocchiaro,
S. Pacetti, P. Patteri, I. M. Peruzzi,[§] M. Piccolo, M. Rama, and A. Zallo
INFN Laboratori Nazionali di Frascati, I-00044 Frascati, Italy

R. Contri[ab], E. Guido, M. Lo Vetere[ab], M. R. Monge[ab], S. Passaggio[a], C. Patrignani[ab], E. Robutti[a], and S. Tosi[ab]
INFN Sezione di Genova[a]; Dipartimento di Fisica, Università di Genova[b], I-16146 Genova, Italy

K. S. Chaisanguanthum and M. Morii
Harvard University, Cambridge, Massachusetts 02138, USA

A. Adametz, J. Marks, S. Schenk, and U. Uwer
Universität Heidelberg, Physikalisches Institut, Philosophenweg 12, D-69120 Heidelberg, Germany

F. U. Bernlochner, V. Klose, and H. M. Lacker
Humboldt-Universität zu Berlin, Institut für Physik, Newtonstr. 15, D-12489 Berlin, Germany

D. J. Bard, P. D. Dauncey, and M. Tibbetts
Imperial College London, London, SW7 2AZ, United Kingdom

P. K. Behera, M. J. Charles, and U. Mallik
University of Iowa, Iowa City, Iowa 52242, USA

J. Cochran, H. B. Crawley, L. Dong, V. Eyges, W. T. Meyer, S. Prell, E. I. Rosenberg, and A. E. Rubin
Iowa State University, Ames, Iowa 50011-3160, USA

Y. Y. Gao, A. V. Gritsan, and Z. J. Guo
Johns Hopkins University, Baltimore, Maryland 21218, USA

N. Arnaud, J. Béquilleux, A. D'Orazio, M. Davier, D. Derkach, J. Firmino da Costa,
G. Grosdidier, F. Le Diberder, V. Lepeltier, A. M. Lutz, B. Malaescu, S. Pruvot,
P. Roudeau, M. H. Schune, J. Serrano, V. Sordini,[¶] A. Stocchi, and G. Wormser
Laboratoire de l'Accélérateur Linéaire, IN2P3/CNRS et Université Paris-Sud 11,
Centre Scientifique d'Orsay, B. P. 34, F-91898 Orsay Cedex, France

D. J. Lange and D. M. Wright
Lawrence Livermore National Laboratory, Livermore, California 94550, USA

I. Bingham, J. P. Burke, C. A. Chavez, J. R. Fry, E. Gabathuler,
R. Gamet, D. E. Hutchcroft, D. J. Payne, and C. Touramanis
University of Liverpool, Liverpool L69 7ZE, United Kingdom

A. J. Bevan, C. K. Clarke, F. Di Lodovico, R. Sacco, and M. Sigamani
Queen Mary, University of London, London, E1 4NS, United Kingdom

G. Cowan, S. Paramesvaran, and A. C. Wren
University of London, Royal Holloway and Bedford New College, Egham, Surrey TW20 0EX, United Kingdom

D. N. Brown and C. L. Davis
University of Louisville, Louisville, Kentucky 40292, USA

A. G. Denig, M. Fritsch, W. Gradl, and A. Hafner
Johannes Gutenberg-Universität Mainz, Institut für Kernphysik, D-55099 Mainz, Germany

K. E. Alwyn, D. Bailey, R. J. Barlow, G. Jackson, G. D. Lafferty, T. J. West, and J. I. Yi
University of Manchester, Manchester M13 9PL, United Kingdom

J. Anderson, C. Chen, A. Jawahery, D. A. Roberts, G. Simi, and J. M. Tuggle
University of Maryland, College Park, Maryland 20742, USA

C. Dallapiccola, E. Salvati, and S. Saremi
University of Massachusetts, Amherst, Massachusetts 01003, USA

R. Cowan, D. Dujmic, P. H. Fisher, S. W. Henderson, G. Sciolla, M. Spitznagel, R. K. Yamamoto, and M. Zhao
Massachusetts Institute of Technology, Laboratory for Nuclear Science, Cambridge, Massachusetts 02139, USA

P. M. Patel, S. H. Robertson, and M. Schram
McGill University, Montréal, Québec, Canada H3A 2T8

A. Lazzaro[ab], V. Lombardo[a], F. Palombo[ab], and S. Stracka
INFN Sezione di Milano[a]; Dipartimento di Fisica, Università di Milano[b], I-20133 Milano, Italy

J. M. Bauer, L. Cremaldi, R. Godang,[**] R. Kroeger, D. J. Summers, and H. W. Zhao
University of Mississippi, University, Mississippi 38677, USA

M. Simard and P. Taras
Université de Montréal, Physique des Particules, Montréal, Québec, Canada H3C 3J7

H. Nicholson
Mount Holyoke College, South Hadley, Massachusetts 01075, USA

G. De Nardo[ab], L. Lista[a], D. Monorchio[ab], G. Onorato[ab], and C. Sciacca[ab]
INFN Sezione di Napoli[a]; Dipartimento di Scienze Fisiche,
Università di Napoli Federico II[b], I-80126 Napoli, Italy

G. Raven and H. L. Snoek
NIKHEF, National Institute for Nuclear Physics and High Energy Physics, NL-1009 DB Amsterdam, The Netherlands

C. P. Jessop, K. J. Knoepfel, J. M. LoSecco, and W. F. Wang
University of Notre Dame, Notre Dame, Indiana 46556, USA

L. A. Corwin, K. Honscheid, H. Kagan, R. Kass, J. P. Morris,
A. M. Rahimi, J. J. Regensburger, S. J. Sekula, and Q. K. Wong
Ohio State University, Columbus, Ohio 43210, USA

N. L. Blount, J. Brau, R. Frey, O. Igonkina, J. A. Kolb, M. Lu,

R. Rahmat, N. B. Sinev, D. Strom, J. Strube, and E. Torrence
University of Oregon, Eugene, Oregon 97403, USA

G. Castelli[ab], N. Gagliardi[ab], M. Margoni[ab], M. Morandin[a],
M. Posocco[a], M. Rotondo[a], F. Simonetto[ab], R. Stroili[ab], and C. Voci[ab]
INFN Sezione di Padova[a]; Dipartimento di Fisica, Università di Padova[b], I-35131 Padova, Italy

P. del Amo Sanchez, E. Ben-Haim, H. Briand, J. Chauveau, O. Hamon,
Ph. Leruste, G. Marchiori, J. Ocariz, A. Perez, J. Prendki, and S. Sitt
Laboratoire de Physique Nucléaire et de Hautes Energies,
IN2P3/CNRS, Université Pierre et Marie Curie-Paris6,
Université Denis Diderot-Paris7, F-75252 Paris, France

L. Gladney
University of Pennsylvania, Philadelphia, Pennsylvania 19104, USA

M. Biasini[ab] and E. Manoni[ab]
INFN Sezione di Perugia[a]; Dipartimento di Fisica, Università di Perugia[b], I-06100 Perugia, Italy

C. Angelini[ab], G. Batignani[ab], S. Bettarini[ab], G. Calderini[ab],[†] M. Carpinelli[ab],[‡] A. Cervelli[ab], F. Forti[ab],
M. A. Giorgi[ab], A. Lusiani[ac], M. Morganti[ab], N. Neri[ab], E. Paoloni[ab], G. Rizzo[ab], and J. J. Walsh[a]
INFN Sezione di Pisa[a]; Dipartimento di Fisica, Università di Pisa[b]; Scuola Normale Superiore di Pisa[c], I-56127 Pisa, Italy

D. Lopes Pegna, C. Lu, J. Olsen, A. J. S. Smith, and A. V. Telnov
Princeton University, Princeton, New Jersey 08544, USA

F. Anulli[a], E. Baracchini[ab], G. Cavoto[a], R. Faccini[ab], F. Ferrarotto[a], F. Ferroni[ab], M. Gaspero[ab],
P. D. Jackson[a], L. Li Gioi[a], M. A. Mazzoni[a], S. Morganti[a], G. Piredda[a], F. Renga[ab], and C. Voena[a]
INFN Sezione di Roma[a]; Dipartimento di Fisica,
Università di Roma La Sapienza[b], I-00185 Roma, Italy

M. Ebert, T. Hartmann, H. Schröder, and R. Waldi
Universität Rostock, D-18051 Rostock, Germany

T. Adye, B. Franek, E. O. Olaiya, and F. F. Wilson
Rutherford Appleton Laboratory, Chilton, Didcot, Oxon, OX11 0QX, United Kingdom

S. Emery, L. Esteve, G. Hamel de Monchenault, W. Kozanecki, G. Vasseur, Ch. Yèche, and M. Zito
CEA, Irfu, SPP, Centre de Saclay, F-91191 Gif-sur-Yvette, France

M. T. Allen, D. Aston, R. Bartoldus, J. F. Benitez, R. Cenci, J. P. Coleman, M. R. Convery,
J. C. Dingfelder, J. Dorfan, G. P. Dubois-Felsmann, W. Dunwoodie, R. C. Field, A. M. Gabareen,
M. T. Graham, P. Grenier, C. Hast, W. R. Innes, J. Kaminski, M. H. Kelsey, H. Kim, P. Kim, M. L. Kocian,
D. W. G. S. Leith, S. Li, B. Lindquist, S. Luitz, V. Luth, H. L. Lynch, D. B. MacFarlane, H. Marsiske,
R. Messner,[*] D. R. Muller, H. Neal, S. Nelson, C. P. O'Grady, I. Ofte, M. Perl, B. N. Ratcliff,
A. Roodman, A. A. Salnikov, R. H. Schindler, J. Schwiening, A. Snyder, D. Su, M. K. Sullivan, K. Suzuki,
S. K. Swain, J. M. Thompson, J. Va'vra, A. P. Wagner, M. Weaver, C. A. West, W. J. Wisniewski,
M. Wittgen, D. H. Wright, H. W. Wulsin, A. K. Yarritu, K. Yi, C. C. Young, and V. Ziegler
SLAC National Accelerator Laboratory, Stanford, California 94309 USA

X. R. Chen, H. Liu, W. Park, M. V. Purohit, R. M. White, and J. R. Wilson
University of South Carolina, Columbia, South Carolina 29208, USA

P. R. Burchat, A. J. Edwards, and T. S. Miyashita
Stanford University, Stanford, California 94305-4060, USA

S. Ahmed, M. S. Alam, J. A. Ernst, B. Pan, M. A. Saeed, and S. B. Zain

State University of New York, Albany, New York 12222, USA

S. M. Spanier and B. J. Wogsland
University of Tennessee, Knoxville, Tennessee 37996, USA

R. Eckmann, J. L. Ritchie, A. M. Ruland, C. J. Schilling, R. F. Schwitters, and B. C. Wray
University of Texas at Austin, Austin, Texas 78712, USA

B. W. Drummond, J. M. Izen, and X. C. Lou
University of Texas at Dallas, Richardson, Texas 75083, USA

F. Bianchi[ab], D. Gamba[ab], and M. Pelliccioni[ab]
INFN Sezione di Torino[a]; Dipartimento di Fisica Sperimentale, Università di Torino[b], I-10125 Torino, Italy

M. Bomben[ab], L. Bosisio[ab], C. Cartaro[ab], G. Della Ricca[ab], L. Lanceri[ab], and L. Vitale[ab]
INFN Sezione di Trieste[a]; Dipartimento di Fisica, Università di Trieste[b], I-34127 Trieste, Italy

V. Azzolini, N. Lopez-March, F. Martinez-Vidal, D. A. Milanes, and A. Oyanguren
IFIC, Universitat de Valencia-CSIC, E-46071 Valencia, Spain

J. Albert, Sw. Banerjee, B. Bhuyan, H. H. F. Choi, K. Hamano, G. J. King,
R. Kowalewski, M. J. Lewczuk, I. M. Nugent, J. M. Roney, and R. J. Sobie
University of Victoria, Victoria, British Columbia, Canada V8W 3P6

T. J. Gershon, P. F. Harrison, J. Ilic, T. E. Latham, G. B. Mohanty, and E. M. T. Puccio
Department of Physics, University of Warwick, Coventry CV4 7AL, United Kingdom

H. R. Band, X. Chen, S. Dasu, K. T. Flood, Y. Pan, R. Prepost, C. O. Vuosalo, and S. L. Wu
University of Wisconsin, Madison, Wisconsin 53706, USA

---

*Deceased
†Now at Temple University, Philadelphia, Pennsylvania 19122, USA
‡Now at Tel Aviv University, Tel Aviv, 69978, Israel
§Also with Università di Perugia, Dipartimento di Fisica, Perugia, Italy
¶Also with Università di Roma La Sapienza, I-00185 Roma, Italy
**Now at University of South Alabama, Mobile, Alabama 36688, USA
††Also with Laboratoire de Physique Nucléaire et de Hautes Energies, IN2P3/CNRS, Université Pierre et Marie Curie-Paris6, Université Denis Diderot-Paris7, F-75252 Paris, France
‡‡Also with Università di Sassari, Sassari, Italy

I. INTRODUCTION

The concept of mass is one of the most intuitive ideas in physics since it is present in everyday human experience. Yet the fundamental nature of mass remains one of the greatest mysteries in physics. The Higgs mechanism is a theoretically appealing way to account for the different masses of elementary particles [1]. The Higgs mechanism implies the existence of at least one new particle called the Higgs boson, which is the only Standard Model (SM) [2] particle yet to be observed. If it is found, its discovery will have a profound effect on our fundamental understanding of matter. A single Standard Model Higgs boson is required to be heavy, with the mass constrained by direct searches to $m_H > 114.4\,\mathrm{GeV}$ [3] and $m_H \neq 170\,\mathrm{GeV}$ [4], and by precision electroweak measurements to $m_H = 129^{+74}_{-49}\,\mathrm{GeV}$ [5].

The Standard Model and the simplest electroweak symmetry breaking scenario suffer from quadratic divergences in the radiative corrections to the mass parameter of the Higgs potential. Several theories beyond the Standard Model that regulate these divergences have been proposed. Supersymmetry [6] is one such model; however, in its simplest form (the Minimal Supersymmetric Standard Model, MSSM) questions of parameter fine-tuning and "naturalness" of the Higgs mass scale remain.

Theoretical efforts to solve unattractive features of MSSM often result in models that introduce additional Higgs fields, with one of them naturally light. For instance, the Next-to-Minimal Supersymmetric Standard Model (NMSSM) [7] introduces a singlet Higgs field. A linear combination of this singlet state with a member of the electroweak doublet produces a *CP*-odd Higgs state A^0 whose mass is not required to be large. Direct searches typically constrain m_{A^0} to be below $2m_b$ [8] making it accessible to decays of Υ resonances. An ideal place to search for such *CP*-odd Higgs would be $\Upsilon \to \gamma A^0$, as originally proposed by Wilczek [9]. A study of the NMSSM parameter space [10] predicts the branching fraction to this final state to be as high as 10^{-4}.

Other new physics models, motivated by astrophysical observations, predict similar light states. One recent example [11] proposes a light axion-like pseudoscalar boson a decaying predominantly to leptons and predicts the branching fraction $\mathcal{B}(\Upsilon \to \gamma\ a)$ to be between 10^{-6}–10^{-5} [11]. Empirical motivation for a light Higgs search comes from the HyperCP experiment [12]. HyperCP observed three anomalous events in the $\Sigma \to p\mu^+\mu^-$ final state, that have been interpreted as a light scalar with mass of 214.3 MeV decaying into a pair of muons [13]. The large datasets available at *BABAR* allow us to place stringent constraints on such models.

If a light scalar A^0 exists, the pattern of its decays would depend on its mass. Assuming no invisible (neutralino) decays [14], for low masses $m_{A^0} < 2m_\tau$, relevant for the HyperCP [12] and axion [11] interpretations, the dominant decay mode should be $A^0 \to \mu^+\mu^-$. Significantly above the tau threshold, $A^0 \to \tau^+\tau^-$ would dominate, and the hadronic decays may also be significant. This analysis searches for the radiative production of A^0 in $\Upsilon(3S)$ decays, with A^0 decaying into muons:

$$\Upsilon(3S) \to \gamma A^0;\ A^0 \to \mu^+\mu^-$$

The current best limit on the branching fraction $\mathcal{B}(\Upsilon \to \gamma A^0)$ with $A^0 \to \mu^+\mu^-$ comes from a measurement by the CLEO collaboration on $\Upsilon(1S)$ [15]. The quoted limits on $\mathcal{B}(\Upsilon(1S) \to \gamma A^0) \times \mathcal{B}(A^0 \to \mu^+\mu^-)$ are in the range (1-20)$\times 10^{-6}$ for $m_{A^0} < 3.6$ GeV. There are currently no competitive measurements at the higher-mass Υ resonances or for the values of m_{A^0} above the $\tau\tau$ threshold.

In the following, we describe a search for a resonance in the dimuon invariant mass distribution for fully reconstructed final state $\Upsilon(3S) \to \gamma(\mu^+\mu^-)$. We assume that the decay width of the resonance is negligibly small compared to experimental resolution, as expected [11, 16] for m_{A^0} sufficiently far from the mass of the η_b [17]. We also assume that the resonance is a scalar (or pseudo-scalar) particle; while significance of any peak does not depend on this assumption, the signal efficiency and, therefore, the extracted branching fractions are computed for a spin-0 particle. In addition, following the recent discovery of the η_b meson in $\Upsilon(3S)$ decays [17], we look for the leptonic decay of the η_b through the chain $\Upsilon(3S) \to \gamma\eta_b$, $\eta_b \to \mu^+\mu^-$. If the recently discovered state is the conventional quark-antiquark η_b meson, its leptonic width is expected to be negligible. Thus, setting a limit on the dimuon branching fraction sheds some light on the nature of the recently discovered state. We assume $\Gamma(\eta_b) = 10\,\mathrm{MeV}$, which is expected in most theoretical models and is consistent with *BABAR* results [17].

II. THE *BABAR* DETECTOR AND DATASET

We search for two-body transitions $\Upsilon(3S) \to \gamma A^0$, followed by decay $A^0 \to \mu^+\mu^-$ in a sample of $(121.8 \pm 1.2) \times 10^6$ $\Upsilon(3S)$ decays collected with the *BABAR* detector at the PEP-II asymmetric-energy e^+e^- collider at the Stanford Linear Accelerator Center. The data were collected at the nominal center-of-mass (CM) energy $E_{\mathrm{cm}} = 10.355\,\mathrm{GeV}$. The CM frame was boosted relative to the detector approximately along the detector's magnetic field axis by $\beta_z = 0.469$.

We use a sample of $78.5\,\mathrm{fb}^{-1}$ accumulated on $\Upsilon(4S)$ resonance ($\Upsilon(4S)$ sample) for studies of the continuum backgrounds; since $\Upsilon(4S)$ is three orders of magnitude broader than $\Upsilon(3S)$, the branching fraction $\Upsilon(4S) \to \gamma A^0$ is

expected to be negligible. For characterization of the background events and selection optimization we also use a sample of $2.4\,\mathrm{fb}^{-1}$ collected 30 MeV below the $\Upsilon(3S)$ resonance.

Since the *BABAR* detector is described in detail elsewhere [18], only the components of the detector crucial to this analysis are summarized below. Charged particle tracking is provided by a five-layer double-sided silicon vertex tracker (SVT) and a 40-layer drift chamber (DCH). Photons and neutral pions are identified and measured using the electromagnetic calorimeter (EMC), which comprises 6580 thallium-doped CsI crystals. These systems are mounted inside a 1.5-T solenoidal superconducting magnet. The Instrumented Flux Return (IFR) forms the return yoke of the superconducting coil, instrumented in the central barrel region with limited streamer tubes, and in the endcap regions with the resistive-plate chambers, for the identification of muons and the detection of clusters produced by neutral hadrons. We use the GEANT [19] software to simulate interactions of particles traversing the *BABAR* detector, taking into account the varying detector conditions and beam backgrounds.

III. EVENT SELECTION

We select events with exactly two oppositely-charged tracks and a single energetic photon with a CM energy $E^*_\gamma \geq 0.5$ GeV. We allow other photons to be present in the event as long as their CM energies are below 0.5 GeV. We assign a muon mass hypothesis to the two tracks (henceforth referred to as muon candidates), and require that they form a geometric vertex with the $\chi^2_{\rm vtx} < 20$ (for 1 degree of freedom), displaced transversely by at most 2 cm from the nominal location of the e^+e^- interaction region. We perform a kinematic fit to the $\Upsilon(3S)$ candidate formed from the two muon candidates and the energetic photon, constraining the CM energy of the $\Upsilon(3S)$ candidate, within the beam energy spread, to the total beam energy $\sqrt{s}$. We also assume that the $\Upsilon(3S)$ candidate originates from the interaction region. The kinematic fit improves the invariant mass resolution of the muon pair. We place a requirement on the kinematic fit $\chi^2_{\Upsilon(3S)} < 39$ (for 6 degrees of freedom), which corresponds to the probability to reject good kinematic fits of less than 10^{-6}. The kinematic fit χ^2, together with a requirement that the total mass of the $\Upsilon(3S)$ candidate is within 2 GeV of $\sqrt{s}$, suppresses background events with more than two muons and a photon in the final state, such as cascade decays $\Upsilon(3S) \to \gamma\chi_b(2P) \to \gamma\gamma\Upsilon(1S) \to \gamma\gamma\mu^+\mu^-$ etc. We further require that the momentum of the dimuon candidate A^0 and the photon direction are back-to-back in the CM frame to within 0.07 radians, and select events in which the cosine of the angle between the muon direction and A^0 direction in the center of mass of A^0 is less than 0.88. We reject events in which neither muon candidate is positively identified in the IFR.

The kinematic selection described above is highly efficient for signal events. After the selection, the backgrounds are dominated by two types of QED processes: "continuum" $e^+e^- \to \gamma\mu^+\mu^-$ events in which a photon is emitted in the initial or final state, and the initial-state radiation (ISR) production of the vector mesons J/ψ, $\psi(2S)$, and $\Upsilon(1S)$, which subsequently decay into muon pairs. In order to suppress contributions from ISR-produced $\rho^0 \to \pi^+\pi^-$ and $\phi \to K^+K^-$ final states in which a pion or a kaon is misidentified as a muon or decays (*e.g.* through $K^+ \to \mu^+\nu_\mu$), we require that both muons are positively identified when we look for A^0 candidates in the range $m_{A^0} < 1.05$ GeV. Finally, when selecting candidate events in the η_b mass region $m_{\mu\mu} \sim 9.39$ GeV, we require that no secondary photon above a CM energy of $E^*_2 = 0.08$ GeV is present in the event; this requirement suppresses decay chains $\Upsilon(3S) \to \gamma_2\chi_b(2S) \to \gamma_1\gamma_2\Upsilon(1S)$, in which the photon γ_2 has a typical CM energy of 100 MeV.

We use Monte Carlo samples generated at 20 values of m_{A^0} over a broad range $0.212 < m_{A^0} \leq 9.5\,\mathrm{GeV}$ of possible A^0 masses to measure selection efficiency for the signal events. The efficiency varies between 24-44%, depending on the dimuon invariant mass.

IV. EXTRACTION OF SIGNAL YIELDS

The invariant mass spectrum for the selected candidates in the $\Upsilon(3S)$ dataset is shown in Fig. 1. We extract the yield of signal events as a function of the assumed mass m_{A^0} in the interval $0.212 \leq m_{A^0} \leq 9.3\,\mathrm{GeV}$ by performing a series of unbinned extended maximum likelihood fits to the distribution of the "reduced mass"

$$m_R = \sqrt{m^2_{\mu\mu} - 4m^2_\mu}\ . \tag{1}$$

The choice of this variable is motivated by the distribution of the *continuum background* from $e^+e^- \to \gamma\mu^+\mu^-$, which is a smooth function of m_R across the entire range of interest, in particular, the region near the kinematic threshold $m_{\mu\mu} \approx 2m_\mu$ ($m_R \approx 0$). Each fit is performed over a small range of m_R around the value expected for a particular m_{A^0}. We use the $\Upsilon(4S)$ sample to determine the probability density functions (PDFs) for the continuum background in each fit window, which agree within statistical uncertainties with Monte Carlo simulations. We use a threshold (hyperbolic) function to describe the background below $m_R < 0.23$ GeV; its parameters are fixed to the

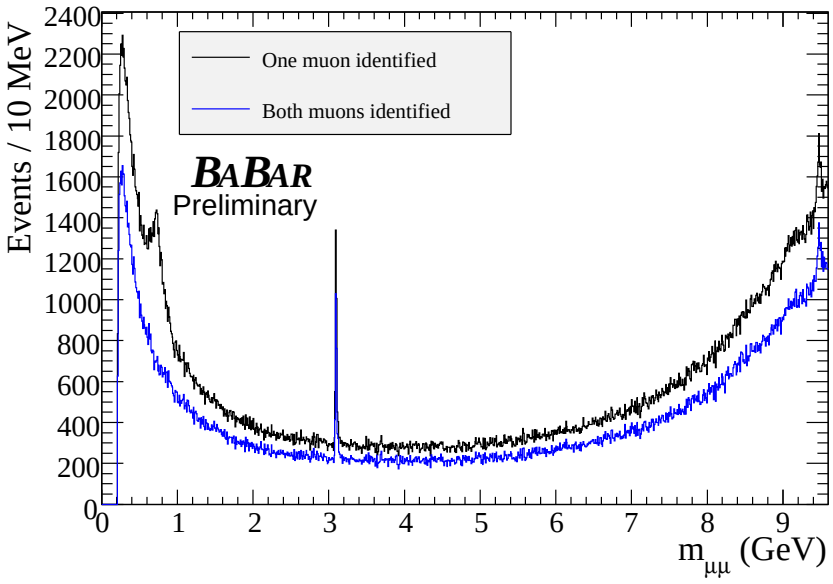

FIG. 1: Distribution of the dimuon invariant mass $m_{\mu^+\mu^-}$ in the $\Upsilon(3S)$ data. Black histogram shows the distribution for the selection in which only one of two muons is required to be positively identified. The peak from $e^+e^- \to \gamma_{\rm ISR}\rho^0(770)$, $\rho^0 \to \pi^+\pi^-$, in which one of the pions is misidentified as a muon, is clearly visible. Blue (lower) histogram shows the distribution for the selection in which both muons are positively identified. The ISR-produced peaks at J/ψ and $\Upsilon(1S)$ masses are visible.

values determined from the fits to the $\Upsilon(4S)$ dataset. Elsewhere the background is well described in each limited m_R range by a first-order ($m_R < 9.3\,\text{GeV}$) or second-order ($m_R > 9.3\,\text{GeV}$) polynomial.

The signal PDF is described by a sum of two Crystal Ball functions [20] with tail parameters on either side of the maximum. The signal PDFs are centered around the expected values of $m_R = \sqrt{m^2_{A^0} - 4m^2_\mu}$ and have the typical resolution of $2-10\,\text{MeV}$, which increases monotonically with m_{A^0}. We determine the PDF as a function of m_{A^0} using a set of high-statistics simulated samples of signal events, and we interpolate PDF parameters and signal efficiency values linearly between simulated points. We determine the uncertainty in the PDF parameters by comparing the distributions of the simulated and reconstructed $e^+e^- \to \gamma_{\rm ISR}J/\psi$, $J/\psi \to \mu^+\mu^-$ events.

Known resonances, such as J/ψ, $\psi(2S)$, and $\Upsilon(1S)$, are present in our sample in specific intervals of m_R, and constitute *peaking background*. We include these contributions in the fit where appropriate, and describe the shape of the resonances using the same functional form as for the signal, a sum of two Crystal Ball functions, with parameters determined from the dedicated MC samples. We do not search for A^0 signal in the immediate vicinity of J/ψ and $\psi(2S)$, ignoring the region of $\approx \pm 40\,\text{MeV}$ around J/ψ (approximately $\pm 5\sigma$) and $\approx \pm 25\,\text{MeV}$ ($\approx \pm 3\sigma$) around $\psi(2S)$.

For each assumed value of m_{A^0}, we perform a likelihood fit to the m_R distribution under the following conditions:

- $0.212 \le m_{A^0} < 0.5\,\text{GeV}$: we use a fixed interval $0.01 < m_R < 0.55\,\text{GeV}$. The fits are done in 2 MeV steps in m_{A^0}. We use a threshold function to describe the combinatorial background PDF below $m_R < 0.23$ GeV, and constrain it to the shape determined from the large $\Upsilon(4S)$ dataset. For $m_R > 0.23$ GeV, we describe the background by a first-order Chebyshev polynomial and float its shape, while requiring continuity at $m_R = 0.23$ GeV. Signal and background yields are free parameters in the fit.

- $0.5 \le m_{A^0} < 1.05\,\text{GeV}$: we use sliding intervals $\mu - 0.2 < m_R < \mu + 0.1\,\text{GeV}$ (where μ is the mean of the signal distribution of m_R). We perform fits in 3 MeV steps in m_{A^0}. First-order polynomial coefficient of the background PDF, signal and background yields are free parameters in the fit.

- $1.05 \le m_{A^0} < 2.9\,\text{GeV}$: we use sliding intervals $\mu - 0.2 < m_R < \mu + 0.1\,\text{GeV}$ and perform fits in 5 MeV steps in m_{A^0}. First-order polynomial coefficient of the background PDF, signal and background yields are free parameters in the fit.

- $2.9 \le m_{A^0} \le 3.055\,\text{GeV}$ and $3.135 \le m_{A^0} \le 3.395\,\text{GeV}$: we use a fixed interval $2.7 < m_R < 3.5\,\text{GeV}$; 5 MeV steps in m_{A^0}. First-order polynomial coefficient of the background PDF, signal, J/ψ, and background yields are free parameters in the fit.

- $3.4 \leq m_{A^0} < 3.55\,\mathrm{GeV}$: we use sliding intervals $\mu - 0.2 < m_R < \mu + 0.1\,\mathrm{GeV}$ and perform fits in 5 MeV steps in m_{A^0}. First-order polynomial coefficient of the background PDF, signal and background yields are free parameters in the fit.

- $3.55 \leq m_{A^0} \leq 3.66\,\mathrm{GeV}$ and $3.71 \leq m_{A^0} < 4.0\,\mathrm{GeV}$: we use fixed interval $3.35 < m_R < 4.1\,\mathrm{GeV}$; 5 MeV steps in m_{A^0}. First-order polynomial coefficient of the background PDF, signal, $\psi(2S)$, and background yields are free parameters in the fit.

- $4.0 \leq m_{A^0} < 9.3\,\mathrm{GeV}$: we use sliding intervals $\mu - 0.2 < m_R < \mu + 0.1\,\mathrm{GeV}$; 5 MeV steps in m_{A^0}. First-order polynomial coefficient of the background PDF, signal and background yields are free parameters in the fit.

- η_b region ($m_{\eta_b} = 9.390\,\mathrm{GeV}$): we use a fixed interval $9.2 < m_R < 9.6\,\mathrm{GeV}$. We constrain the contribution from $e^+e^- \to \gamma_{\mathrm{ISR}}\Upsilon(1S)$ to the expectation from the $\Upsilon(4S)$ dataset (436 ± 50 events). Background PDF shape (second-order Chebyshev polynomial), yields of $\Upsilon(3S) \to \gamma\chi_b(2P) \to \gamma\gamma\Upsilon(1S)$, signal $\Upsilon(3S) \to \gamma\eta_b$ events, and background yields are free parameters in the fit.

The step sizes in each interval correspond approximately to the resolution in m_{A^0}.

As a crosscheck, we also perform a set of two-dimensional maximum likelihood fits to the joint distribution of m_R and $\cos\theta^*_{\mu\mu}$, where $\theta^*_{\mu\mu}$ is the CM polar angle of the dimuon pair. For scalar A^0, the angular distribution of the signal events is expected to be $1 + \cos^2\theta^*_{\mu\mu}$, modulo acceptance and efficiency effects. The distribution of the most dominant QED backgrounds is more strongly peaked in the forward and backward directions. Thus, the angular distribution can help distinguish any signal peaks from the QED background. We find that the results of the two-dimensional fit are consistent with the one-dimensional fit to m_R only.

V. SYSTEMATIC UNCERTAINTIES

The largest systematic uncertainty in $\mathcal{B}(\Upsilon(3S) \to \gamma A^0)$ comes from the measurement of the selection efficiency. We compare the overall selection efficiency between the data and the Monte Carlo simulation by measuring the absolute cross section $d\sigma/dm_R$ for the radiative QED process $e^+e^- \to \gamma\mu^+\mu^-$ over the broad kinematic range $0 < m_R \leq 9.6\,\mathrm{GeV}$, using a sample of $2.4\,\mathrm{fb}^{-1}$ collected 30 MeV below the $\Upsilon(3S)$. We use the ratio of measured to expected cross sections to correct the signal selection efficiency as a function of m_{A^0}. This correction reaches up to 20% at low values of m_{A^0}. We use half of the applied correction, or its statistical uncertainty of 2%, whichever is larger, as the systematic uncertainty on the signal efficiency. This uncertainty accounts for effects of selection efficiency, reconstruction efficiency (for both charged tracks and the photon), trigger efficiency, and the uncertainty in estimating the integrated luminosity. We find the largest difference between the data and Monte Carlo simulation in modeling of muon identification efficiency.

We determine the uncertainty in the signal and peaking background PDFs by comparing the data and simulated distributions of $e^+e^- \to \gamma_{\mathrm{ISR}}J/\psi$ events. We correct for the observed 24% difference (5.3 MeV in the simulations versus 6.6 MeV in the data) in the width of the m_R distribution for these events, and use half of the correction to estimate the systematic uncertainty on the signal yield. This is the dominant systematic uncertainty on the signal yield for $m_{A^0} > 0.4$ GeV. Likewise, we find that changes in the tail parameters of the Crystal Ball PDF describing the J/ψ peak lead to variations in event yield of less than 1%. We use this estimate as a systematic error in the signal yield due to uncertainty in tail parameters.

We find excellent agreement in the shape of the continuum background distributions for $m_R < 0.23$ GeV between $\Upsilon(3S)$ and $\Upsilon(4S)$ data. We determine the PDF in the fits to $\Upsilon(4S)$ data, and propagate their uncertainties to the $\Upsilon(3S)$ data, where these contributions do not exceed $\sigma(\mathcal{B}) = 0.3 \times 10^{-6}$. For the higher masses $m_R > 0.23$ GeV, the background PDF parameters are floated in the likelihood fit.

We test for possible bias in the fitted value of the signal yield with a large ensemble of pseudo-experiments. For each experiment, we generate a sample of background events according to the number and the PDF observed in the data, and add a pre-determined number of signal events from fully-reconstructed signal Monte Carlo samples. The bias is consistent with zero for all values of m_{A^0}, and we assign a branching fraction uncertainty of $\sigma(\mathcal{B}) = 0.02 \times 10^{-6}$ at all values of m_{A^0} to cover the statistical variations in the results of the test.

The uncertainties in PDF parameters of both signal and background and the bias uncertainty affect the signal yield (and therefore significance of any peak); signal efficiency uncertainty does not. The effect of the systematic uncertainties on the signal yield is generally small. The statistical and systematic uncertainties on the branching fraction $\mathcal{B}(\Upsilon(3S) \to \gamma A^0)$ as a function of m_{A^0} are shown in Fig. 2.

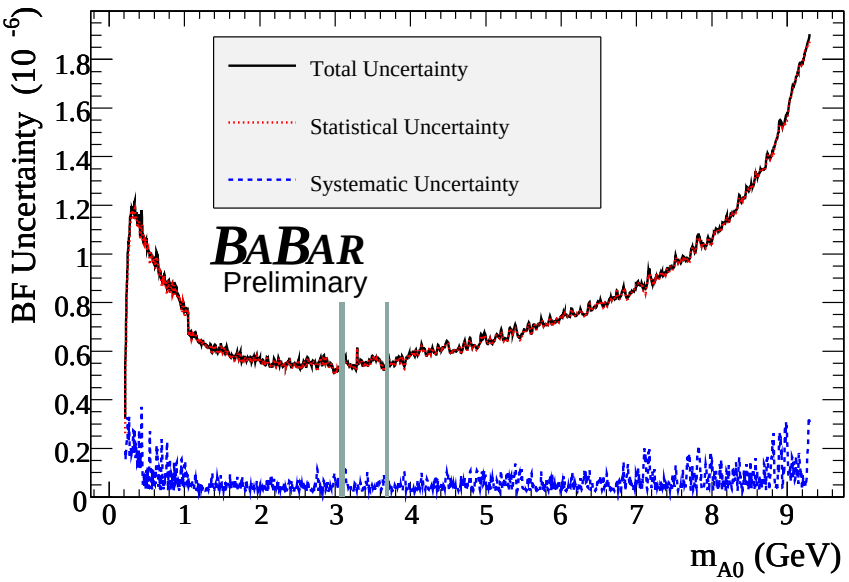

FIG. 2: Statistical and systematic uncertainty on the product of branching fractions $\mathcal{B}(\Upsilon(3S) \to \gamma A^0) \times \mathcal{B}(A^0 \to \mu^+\mu^-)$ as a function of m_{A^0}, extracted from the fits to the $\Upsilon(3S)$ data. Statistical errors are shown as red dot-dashed line, systematic uncertainties are shown as blue dotted line, and the total uncertainty, computed as a quadrature sum of statistical and systematic errors, is the solid black line. The shaded areas show the regions around the J/ψ and $\psi(2S)$ resonances excluded from the search.

VI. STATISTICAL INTERPRETATION

In the event of a positive observation, statistical significance of a particular peak needs to be assessed. Conventionally, this is done by computing the likelihood ratio variable

$$\mathcal{S}(m_{A^0}) = \sqrt{2\log(L_{\rm max}/L_0)} \tag{2}$$

where $L_{\rm max}$ is the maximum likelihood value for a fit with a floated signal yield centered at m_{A^0}, and L_0 is the value of the likelihood for the fixed zero signal yield. Under the null hypothesis (no signal events in the data), the signed quantity, $sign(N_{\rm sig})\mathcal{S}$ is expected to be normal-distributed (where $N_{\rm sig}$ is the fitted signal yield). The distribution for our $\Upsilon(3S)$ dataset is shown in Fig. 3. Since our scans have $\mathcal{O}(2000)$ m_{A^0} points, we should expect several statistical fluctuations at the level of $\mathcal{S} \approx 3$, even for a null signal hypothesis.

For a single experiment consisting of $N_{\rm trial}$ uncorrelated measurements, the probability to observe $\mathcal{S} \geq \mathcal{S}_{\rm max}$ and $N_{\rm sig} > 0$ is

$$P(\mathcal{S}_{\rm max}; N_{\rm trial}) \approx N_{\rm trial} P(\mathcal{S}_{\rm max}; 1) = N_{\rm trial} \frac{{\rm Erfc}(\mathcal{S}_{\rm max}/\sqrt{2})}{2} \tag{3}$$

(this approximation is good for $P(\mathcal{S}_{\rm max}; N_{\rm trial}) \ll 1$). The "trial factor" $N_{\rm trial}$ is difficult to estimate analytically. Instead, we determine $N_{\rm trial}$ by inspecting results of 10^8 Monte Carlo pseudo-experiments; for each experiment we generate 1951 random values x_i according to

$$x_i = x_{i-1}\rho + r\sqrt{1-\rho^2} \tag{4}$$

where $\rho = 0.84$ is the average correlation coefficient between adjacent "bins" x_i and x_{i-1}, as determined by $\Upsilon(3S)$ fits, and r is a normal-distributed random number. We then compute the maximum value $\mathcal{S}_{\rm max}$ for each pseudo-experiment. The cumulative distribution of $\mathcal{S}_{\rm max}$ describes the chance that a pure background would fluctuate to produce a signal peak *at any value* of m_{A^0} with the likelihood ratio variable $\mathcal{S} \geq \mathcal{S}_{\rm max}$. From the fit to the distribution of $\mathcal{S}_{\rm max}$ from 10^8 pseudo-experiments, we determine the effective trial factor $N_{\rm trial} = 1436 \pm 16$. Finally, we convert the likelihood ratio variable $\mathcal{S}$ to the true statistical significance $\mathcal{S}^{'}$ in terms of gaussian σ:

$$\mathcal{S}^{'} \approx \sqrt{2}{\rm Erfc}^{-1}\left[N_{\rm trial}{\rm Erfc}(\mathcal{S}_{\rm max}/\sqrt{2})\right] \;\; (\mathcal{S} > 4) \tag{5}$$

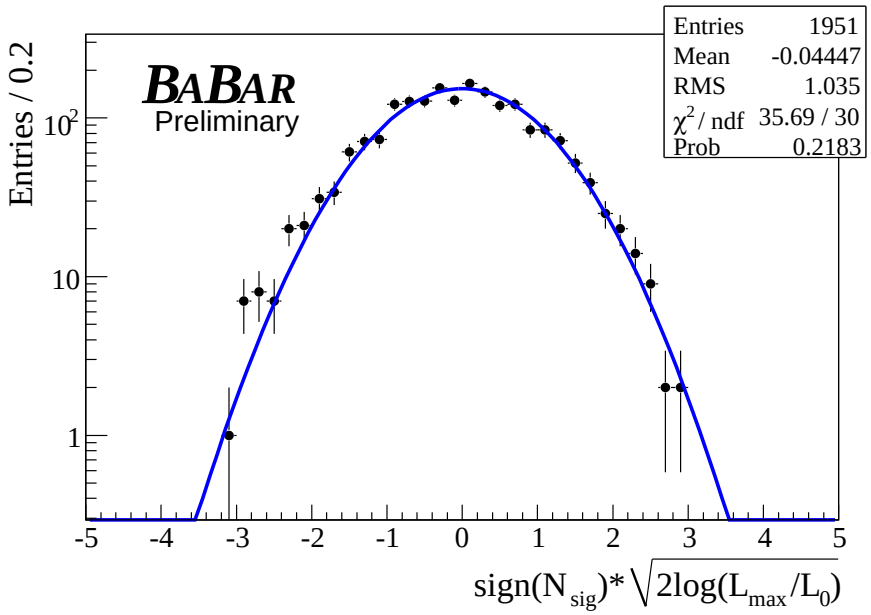

FIG. 3: Distribution of the likelihood ratio variable $\mathcal{S}$ (with additive systematic uncertainties included for the fits to the $\Upsilon(3S)$ dataset. The blue curve is the Gaussian fit with fixed $\mu = 0$ and $\sigma = 1$.

In particular, the threshold for observing "evidence" for signal at *any* value of m_{A^0} is $\mathcal{S}^{'} \geq 3.0$; this corresponds to the likelihood ratio at a *particular* value of m_{A^0} of $\mathcal{S} \geq 4.8$.

VII. RESULTS AND CONCLUSIONS

For a small number of fits in the scan over the $\Upsilon(3S)$ dataset, we observe local likelihood ratio values $\mathcal{S}$ of about 3σ. The most significant peak is at $m_{A^0} = 4.940 \pm 0.003$ GeV (likelihood ratio value $\mathcal{S} = 3.0$, including systematics; $\mathcal{B} = (1.9 \pm 0.7 \pm 0.1) \times 10^{-6}$). The second most-significant peak is at $m_{A^0} = 0.426 \pm 0.001$ GeV (likelihood ratio value $\mathcal{S} = 2.9$, including systematics; $\mathcal{B} = (3.1 \pm 1.1 \pm 0.3) \times 10^{-6}$). The plots for these points are shown in Fig. 4 and Fig. 5. The peak at $m_{A^0} = 4.940$ GeV is theoretically disfavored (since it is significantly above the τ threshold), while the peak at $m_{A^0} = 0.426$ GeV is in the range predicted by the axion model [11]. Neither of the peaks are significant, however, when we take into account the trial factor discussed in Section VI. At least 80% of our pseudo-experiments contain a fluctuation with $\mathcal{S} = 3\sigma$ or more.

Since we do not observe a significant excess of events above the background in the range $0.212 < m_{A^0} \leq 9.3\,\text{GeV}$, we set upper limits on the branching fraction $\mathcal{B}(\Upsilon(3S) \to \gamma A^0) \times \mathcal{B}(A^0 \to \mu^+\mu^-)$. We add statistical and systematic uncertainties (which include the additive errors on the signal yield and multiplicative uncertainties on the signal efficiency and the number of recorded $\Upsilon(3S)$ decays) in quadrature. The 90% C.L. Bayesian upper limits, computed with a uniform prior and assuming a Gaussian likelihood function, are shown in Fig. 6-9 as a function of mass m_{A^0}. The limits fluctuate depending on the central value of the signal yield returned by a particular fit, and range from 0.25×10^{-6} to 5.2×10^{-6}.

We do not observe any significant signal at the HyperCP mass, $m_{A^0} = 0.214$ GeV (see Fig. 10). We find $\mathcal{B}(\Upsilon(3S) \to \gamma A^0(214)) = (0.12^{+0.43}_{-0.41} \pm 0.17) \times 10^{-6}$, and set an upper limit $\mathcal{B}(\Upsilon(3S) \to \gamma A^0(214)) < 0.8 \times 10^{-6}$ at 90% C.L.

A fit to the η_b region is shown in Fig. 11. We find $\mathcal{B}(\Upsilon(3S) \to \gamma\eta_b) \times \mathcal{B}(\eta_b \to \mu^+\mu^-) = (0.2 \pm 3.0 \pm 0.9) \times 10^{-6}$, consistent with zero. Taking into account the *BABAR* measurement of $\mathcal{B}(\Upsilon(3S) \to \gamma\eta_b) = (4.8 \pm 0.5 \pm 1.2) \times 10^{-4}$, we can derive $\mathcal{B}(\eta_b \to \mu^+\mu^-) = (0.0 \pm 0.6 \pm 0.2)\%$, or an upper limit $\mathcal{B}(\eta_b \to \mu^+\mu^-) < 0.8\%$ at 90% C.L. This is consistent with expectations from the quark model. All results above are preliminary.

The limits we set are more stringent than those reported by the CLEO collaboration recently [15]. Our limits rule out much of the parameter space allowed by the light Higgs [10] and axion [11] models.

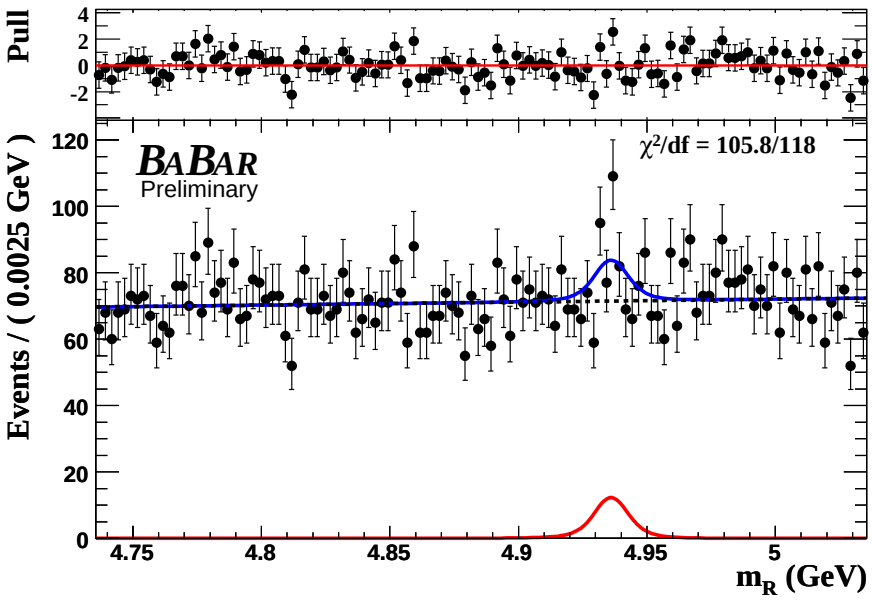

FIG. 4: The fit for $m_{A^0} = 4.940$ GeV in $\Upsilon(3S)$ dataset. The bottom graph shows the m_R distribution (solid points), overlaid by the full PDF (solid blue line). Also shown are the contributions from the signal at $m_{A^0} = 4.940$ GeV (solid red line) and the continuum background (dashed black line). The top plot shows the normalized residuals $p = (\text{data}-\text{fit})/\sigma(\text{data})$ with unit error bars. The signal peak corresponds to the likelihood ratio variable $\mathcal{S} = 3.0$, including systematics, and $\mathcal{B} = (1.9\pm0.7\pm0.1)\times10^{-6}$.

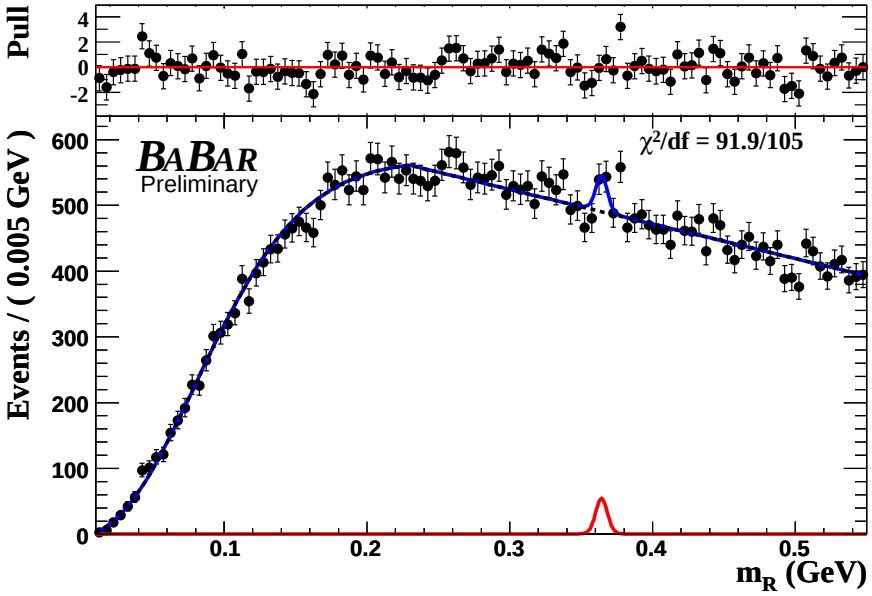

FIG. 5: The fit for $m_{A^0} = 0.426$ GeV in $\Upsilon(3S)$ dataset. The bottom graph shows the m_R distribution (solid points), overlaid by the full PDF (solid blue line). Also shown are the contributions from the signal at $m_{A^0} = 0.426$ GeV (solid red line) and the continuum background (dashed black line). The top plot shows the normalized residuals $p = (\text{data}-\text{fit})/\sigma(\text{data})$ with unit error bars. The signal peak corresponds to the likelihood ratio variable $\mathcal{S} = 2.9$, including systematics, and $\mathcal{B} = (3.1\pm1.1\pm0.3)\times10^{-6}$.

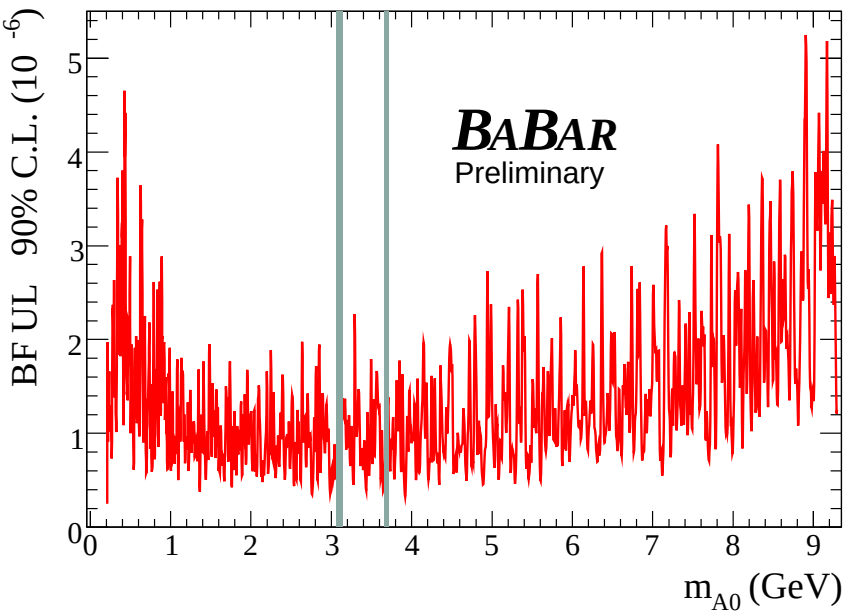

FIG. 6: Upper limits on the product of branching fractions $\mathcal{B}(\Upsilon(3S) \to \gamma A^0) \times \mathcal{B}(A^0 \to \mu^+\mu^-)$ as a function of m_{A^0} from the fits to $\Upsilon(3S)$ data. The shaded areas show the regions around the J/ψ and $\psi(2S)$ resonances excluded from the search.

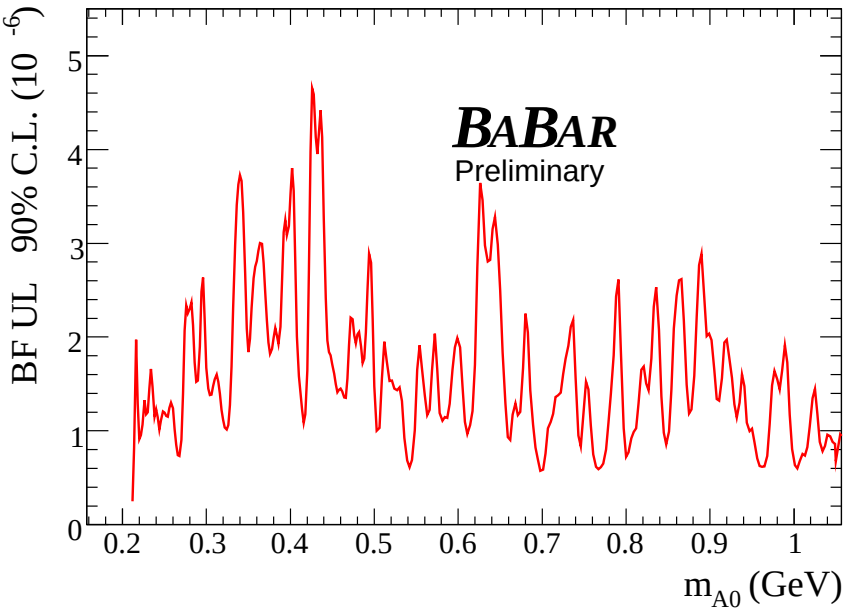

FIG. 7: Upper limits on the product of branching fractions $\mathcal{B}(\Upsilon(3S) \to \gamma A^0) \times \mathcal{B}(A^0 \to \mu^+\mu^-)$ as a function of m_{A^0} in the range $0.212 \leq m_{A^0} \leq 1.05$ GeV from the fits to $\Upsilon(3S)$ data.

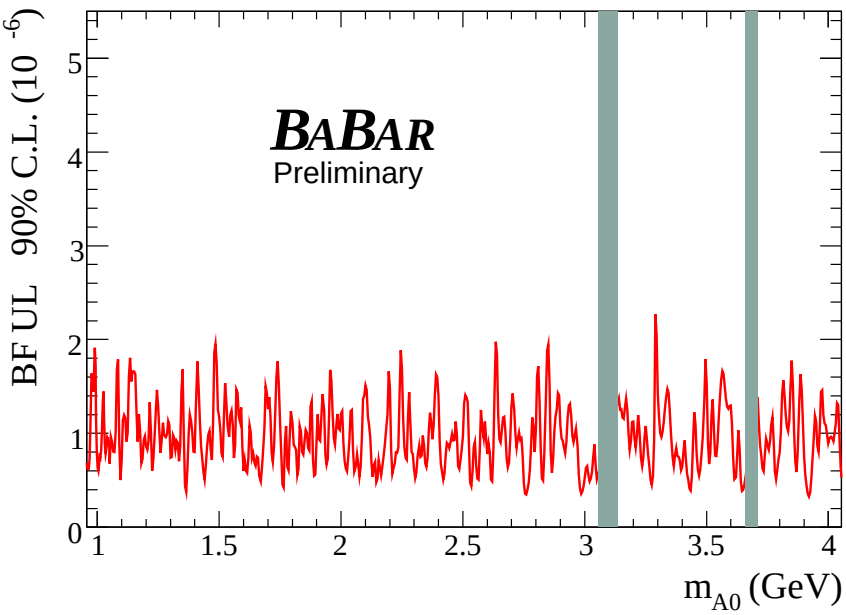

FIG. 8: Upper limits on the product of branching fractions $\mathcal{B}(\Upsilon(3S) \to \gamma A^0) \times \mathcal{B}(A^0 \to \mu^+\mu^-)$ as a function of m_{A^0} in the range $1 \leq m_{A^0} \leq 4$ GeV from the fits to $\Upsilon(3S)$ data. The shaded areas show the regions around the J/ψ and $\psi(2S)$ resonances excluded from the search.

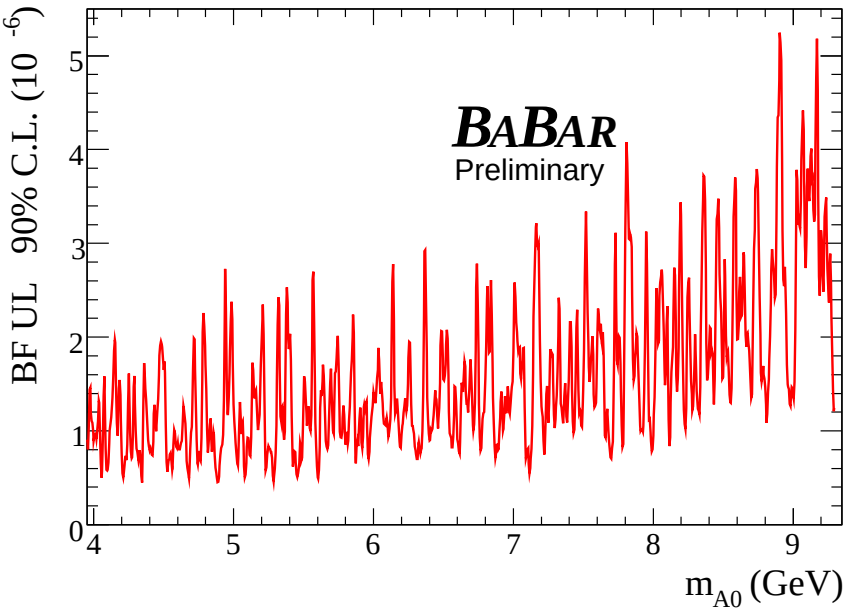

FIG. 9: Upper limits on the product of branching fractions $\mathcal{B}(\Upsilon(3S) \to \gamma A^0) \times \mathcal{B}(A^0 \to \mu^+\mu^-)$ as a function of m_{A^0} in the range $4 \leq m_{A^0} \leq 9.3$ GeV from the fits to $\Upsilon(3S)$ data.

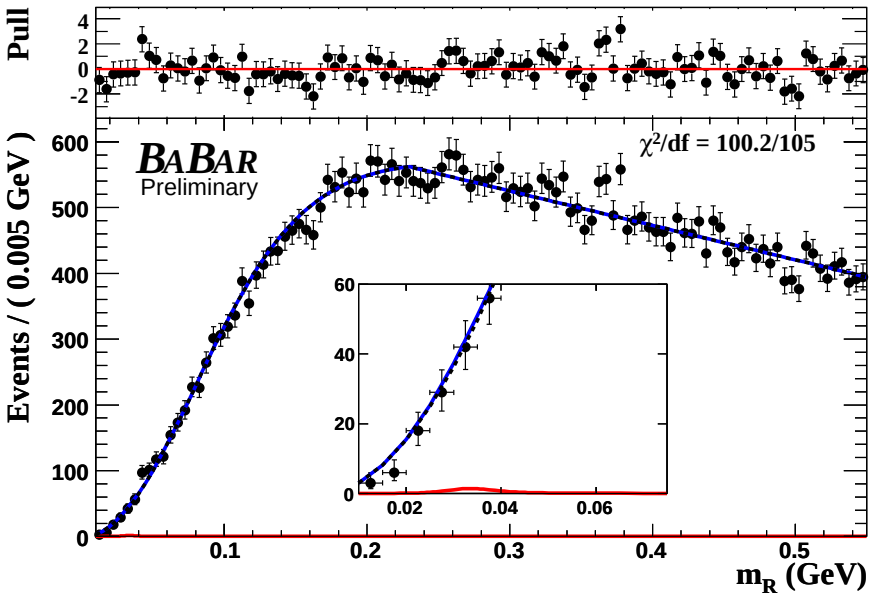

FIG. 10: The fit for $m_{A^0} = 0.214$ GeV (HyperCP candidate) in the $\Upsilon(3S)$ dataset. The bottom graph shows the m_R distribution (solid points), overlaid by the full PDF (solid blue line). Also shown are the contributions from the signal at $m_{A^0} = 0.214$ GeV (solid red line) and the continuum background (dashed black line). The inset zooms in on the HyperCP region of interest. The top plot shows the normalized residuals $p = (\text{data} - \text{fit})/\sigma(\text{data})$ with unit error bars.

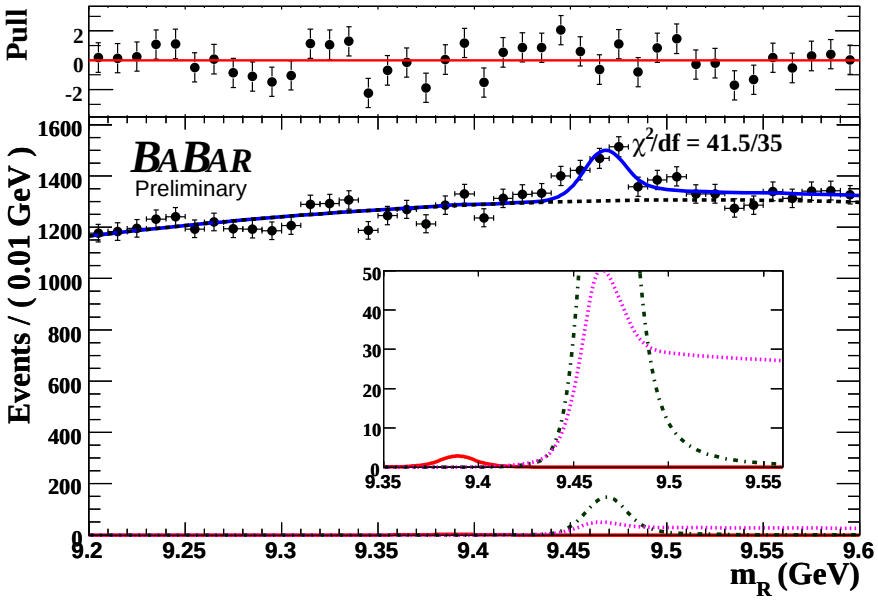

FIG. 11: The fit for the η_b region in $\Upsilon(3S)$ dataset. The bottom graph shows the m_R distribution (solid points), overlaid by the full PDF (solid blue line). Also shown are the contributions from the signal at at $m_{\eta_b} = 9.389$ GeV (solid red line), background from the $e^+e^- \to \gamma_{\rm ISR}\Upsilon(1S)$ (dot-dashed green line), background from $\Upsilon(3S) \to \gamma\chi_b(2P)$, $\chi_b(2P) \to \gamma\Upsilon(1S)$ (dotted magenta line), and the continuum background (dashed black line). The inset shows the signal, $e^+e^- \to \gamma_{\rm ISR}\Upsilon(1S)$, and $\chi_b(2P) \to \gamma\Upsilon(1S)$ in more detail. The top plot shows the normalized residuals $p = (\text{data} - \text{fit})/\sigma(\text{data})$ with unit error bars.

VIII. ACKNOWLEDGMENTS

We are grateful for the extraordinary contributions of our PEP-II colleagues in achieving the excellent luminosity and machine conditions that have made this work possible. The success of this project also relies critically on the expertise and dedication of the computing organizations that support *BABAR*. The collaborating institutions wish to thank SLAC for its support and the kind hospitality extended to them. This work is supported by the US Department of Energy and National Science Foundation, the Natural Sciences and Engineering Research Council (Canada), the Commissariat à l'Energie Atomique and Institut National de Physique Nucléaire et de Physique des Particules (France), the Bundesministerium für Bildung und Forschung and Deutsche Forschungsgemeinschaft (Germany), the Istituto Nazionale di Fisica Nucleare (Italy), the Foundation for Fundamental Research on Matter (The Netherlands), the Research Council of Norway, the Ministry of Education and Science of the Russian Federation, Ministerio de Educación y Ciencia (Spain), and the Science and Technology Facilities Council (United Kingdom). Individuals have received support from the Marie-Curie IEF program (European Union) and the A. P. Sloan Foundation.

We thank Radovan Dermisek, Jack Gunion, Zoltan Ligeti, Yasunori Nomura, Miguel Sanchis-Lozano, and Jesse Thaler for stimulating discussions.

---

[1] P.W. Higgs Phys. Rev. Lett. **13**, 508 (1964).
[2] S. Weinberg, Phys. Rev. Lett. **19**, 1264 (1967); A. Salam, p. 367 of *Elementary Particle Theory*, ed. N. Svartholm (Almquist and Wiksells, Stockholm, 1969); S.L. Glashow, J. Iliopoulos, and L. Maiani, Phys. Rev. D **2**, 1285 (1970).
[3] LEP Working Group for Higgs boson searches, R. Barate *et al.*, Phys. Lett. **B565**, 61 (2003).
[4] M. Herndon, rapporteur talk at ICHEP '08, arXiv:0810.3705 [hep-ex] (2008).
[5] LEP-SLC Electroweak Working Group, Phys. Rept. **427**, 257 (2006).
[6] J. Wess and B. Zumino, Nucl. Phys. **B70**, 39 (1974).
[7] R. Dermisek and J.F. Gunion, Phys. Rev. Lett. **95**, 041801 (2005).
[8] R. Dermisek and J.F. Gunion, Phys. Rev. D **73**, 111701 (2006).
[9] F. Wilczek, Phys. Rev. Lett. **39**, 1304 (1977).
[10] R. Dermisek, J.F. Gunion, and B. McElrath, Phys. Rev. D **76**, 051105 (2007).
[11] Y. Nomura and J. Thaler, preprint arXiv:0810.5397 [hep-ph] (2008).
[12] H. Park *et al.*, HyperCP Collaboration Phys. Rev. Lett. **94**, 021801 (2005).
[13] X. G. He, J. Tandean and G. Valencia, Phys. Rev. Lett. **98**, 081802 (2007).
[14] *BABAR* Collaboration, B. Aubert *et al.*, preprint arXiv:0808.0017 [hep-ex] (2008).
[15] CLEO Collaboration, W. Love, *et al.*, Phys. Rev. Lett. **101**, 151802 (2008).
[16] E. Fullana and M.A. Sanchis-Lozano, Phys. Lett. B **653**, 67 (2007).
[17] *BABAR* Collaboration, B. Aubert *et al.*, Phys. Rev. Lett. **101**, 071801 (2008).
[18] *BABAR* Collaboration, B. Aubert *et al.*, Nucl. Instrum. Methods Phys. Res., Sect. A **479**, 1 (2002).
[19] GEANT4 Collaboration, S. Agostinelli *et al.*, Nucl. Instrum. Methods Phys. Res., Sect. A **506**, 250 (2003).
[20] M. J. Oreglia, Ph.D Thesis, report SLAC-236 (1980), Appendix D; J. E. Gaiser, Ph.D Thesis, report SLAC-255 (1982), Appendix F; T. Skwarnicki, Ph.D Thesis, report DESY F31-86-02(1986), Appendix E.